Hue University Journal of Science: Natural Science
Vol. 130, No. 1B, 13–20, 2021

pISSN 1859-1388
eISSN 2615-9678

SINTERING BEHAVIOR AND PHYSICAL PROPERTIES OF $Bi_{0.5}(Na_{1-x}K_x)_{0.5}SnO_3$ LEAD-FREE CERAMICS

Nguyen Truong Tho[1]*, Le Ngoc Minh[1], Le Tran Uyen Tu[1], Dung Thi Hoai Trang[1], Le Phuoc Dinh[1], Nguyen Ly Huu Huan[1], Le Thi Phuong Thao[1,2], Nguyen Thi Hue[1,3], Ngo Minh Hau[1,4]

[1] University of Sciences, Hue University, 77 Nguyen Hue St., Hue, Vietnam
[2] Danang University of Education, The University of Danang, 459 Ton Duc Thang St., Lien Chieu Dist., Danang, Vietnam
[3] Nguyen Tat Thanh Junior-High School, 9 Nguyen Hue St., Kon Tum City, Kon Tum, Vietnam
[4] Nguyen Hue Junior-High School, 9 Hoang Dieu St., Tuy Hoa City, Tuy Hoa, Vietnam

* Correspondence to Nguyen Truong Tho <nttho@hueuni.edu.vn>

(*Received: 22 February 2021; Accepted: 7 May 2021*)

Abstract. In this study, $Bi_{0.5}(Na_{1-x}K_x)_{0.5}SnO_3$ (BNKS) ceramics (x = 0, 0.1, 0.2, 0.3, and 0.4) were fabricated via ultrasound wave before milling. The time of ball milling decreased from 20 to 1 h. The X-ray diffraction patterns show that the BNKS has a single-phase structure. When the potassium content increases, the phase structure of the ceramics changes from rhombohedral to tetragonal. When sintered at 1100 °C and x = 0.2, the ceramics' physical properties are the best with the mass density of 5.59 g/cm^3, the electromechanical coupling constants k_p of 0,31 and k_t of 0.27, the remanent polarization of 11.9 μC/cm; the dielectric constant ε_r of 1131, and the highest dielectric constant ε_{max} of 4800.

Keywords: Lead-free ceramics, BNKS, electromechanical coupling factor, sintering, dielectric constant

1 Introduction

The study and application of ferroelectric and piezoelectric ceramics and/or thin films based on PZT have recently been conducted because of the good piezoelectric properties of these materials [1-3]. However, lead-based materials have caused numerous environmental and human health concerns due to the toxicity of lead oxide. Therefore, developing lead-free ceramics and thin film with piezoelectric and ferroelectric properties is of great importance [4-11].

Improving physical properties and reducing sintering temperatures to limit evaporation are two solutions to fabricate lead-free ceramics. The most common way to enhance physical properties is to combine at least two materials with a perovskite ABO_3 structure into a multi-component material system at the morphology phase boundary. In addition, for reducing sintering temperatures, selecting the ceramics' proportions to form a liquid phase during sintering is an effective way. In reality, $Bi_{0.5}(Na_{0.8}K_{0.2})_{0.5}TiO_3$ piezoelectric ceramics with promising ferroelectric and piezoelectric properties have been studied and fabricated [12-17]. However, when Ti^{4+} is combined with Bi^{3+}, Na^+, and K^+, a liquid phase does not form during sintering. In contrast, Sn^{4+} can form a liquid phase with Bi^{3+} at the Eutectic temperature of about 170 °C [18]. Therefore, it is necessary to replace Ti^{4+} with Sn^{4+} or the fabrication of $Bi_{0.5}(Na_{1-x}K_x)_{0.5}SnO_3$ (BNKS) piezoelectric ceramics with variable x to determine the morphology phase boundary between $Bi_{0.5}Na_{0.5}SnO_3$ (BNS) and $Bi_{0.5}K_{0.5}SnO_3$ (BKS).

2 Experimental

$Bi_{0.5}(Na_{1-x}K_x)_{0.5}SnO_3$ ceramics, where x = 0, 0.1, 0.2, 0.3, and 0.4, were fabricated from Bi_2O_3 (Merck, 99.5%) Na_2CO_3 (Merck, 99.1%), K_2CO_3 (Merck, 99.1%) and SnO_2 (Merck, 99.6%). The ceramics were produced with the help of ultrasound wave before milling (Fig. 1).

First, Bi_2O_3, Na_2CO_3, K_2CO_3, and SnO_2 were weighed and made smooth with ultrasound (an electric power of 100 W and fixed frequency 28 kHz) in ethanol for one hour. This smoothing technique reduces the time of ball milling from 20 to 1 h [18]. The fine powder was then dried and calcined at 850 °C for 2 h to form BNKS proportions. The BNKS proportions were obtained after the ultrasound and solid-phase reactions according to Eq. (1).

The differential thermal analysis (DTA) and the thermogravimetric analysis (TGA) of BNKS powder, performed at a heating rate of 10 °C/min, show that the phase formation reaction occurs at 823.25 °C (Fig. 2). Therefore, we chose 850 °C as the calcination temperature to ensure that every location in the sample has a temperature of more than 823.25 °C.

The calcined BNKS powder was finely milled for 16 h and pressed in the form of a plate cylinder of a 12 mm diameter and 1.5 mm thickness under a pressure of 100 MPa. The samples were then sintered at 1000, 1050, 1100, and 1150 °C for 2 h.

$$Bi_2O_3 + (1-x)Na_2CO_3 + xK_2CO_3 + 4SnO_2 \rightarrow 4Bi_{0.5}(Na_{1-x}K_x)_{0.5}SnO_3 + CO_2 \quad (1)$$

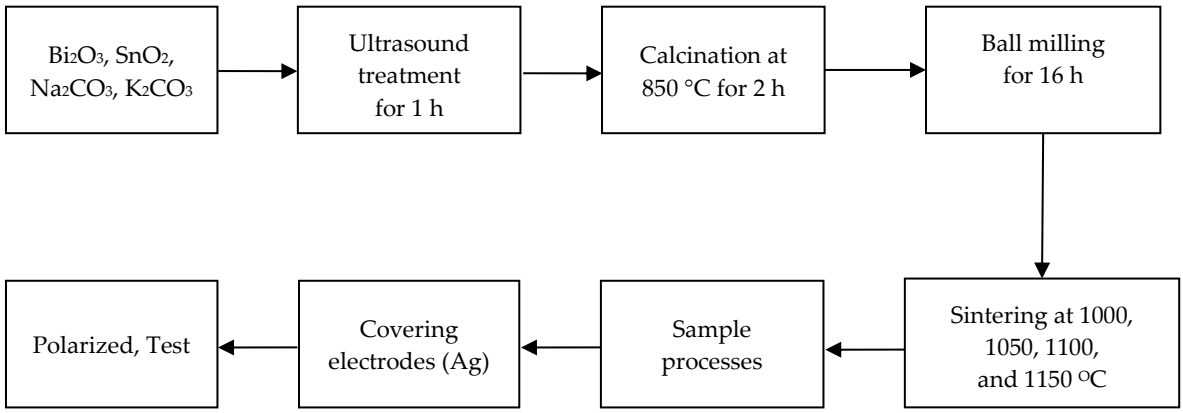

Fig. 1. Process of fabrication technology of $Bi_{0.5}(Na_{1-x}K_x)_{0.5}SnO_3$ ceramics

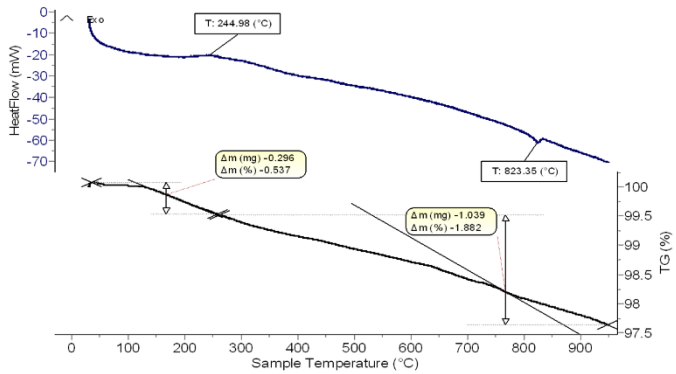

Fig. 2. TG and DTA curves of BNKS powder at 10 °C/min heating rate

pISSN 1859-1388
eISSN 2615-9678

The BNKS crystal structure was investigated with X-ray diffraction spectrometry (XRD) at room temperature. The surface morphology of the ceramic samples was determined with field-emission scanning electron microscopy (FESEM; JSM – 6340F), and the density of the ceramics was measured with the Archimedes method. The piezoelectric properties were determined with the resonance method according to the IEEE Standard 61M on an impedance analyzer Agilent 4196B and RLC. The ferroelectric properties were studied with the Sawyer-Tower method.

3 Results and discussion

Fig. 3 shows the mass density of BNKS ceramic samples at different sintering temperatures. When potassium is absent (x = 0), the ceramic has the highest density at 1150 °C (5.14 g/cm^3). In contrast, when potassium is incorporated in the ceramic, the material exhibits the highest density (5.59 g/cm^3) when sintered at 1100 °C and x = 0.2. This fact proves that the combination of BNS and BKS reduces the sintering temperature, leading to limited evaporation of Bi_2O_3 at high temperatures [18].

Fig. 4 shows the effect of sintering temperatures on the dielectric constant ε and the dielectric loss of tanδ of $Bi_{0.5}(Na_{0.8}K_{0.2})_{0.5}SnO_3$ ceramics, measured at room temperature at 1 kHz. Accordingly, the dielectric constant increases with the increase in the sintering temperature and reaches the highest value (ε = 1131) at 1100 °C and then decreases gradually. This decrease can be explained via the largest particle size and the density of the ceramics, as shown in Fig. 5. The larger the particle size is, the larger is the domain with smaller domain boundaries. These changes limit the cracks inside the sample. However, when the temperature is higher than 1100 °C, the particle size remains constant. Still, the evaporation of Bi_2O_3 during sintering at high temperatures would deteriorate the dielectric properties of the ceramics. Therefore, the sintering temperature of 1100 °C is chosen for further experiments.

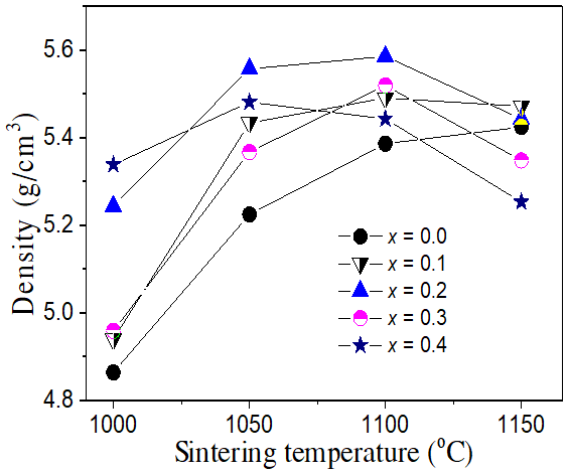

Fig. 3. Mass density of $Bi_{0.5}(Na_{1-x}K_x)_{0.5}SnO_3$ ceramics at different sintering temperatures

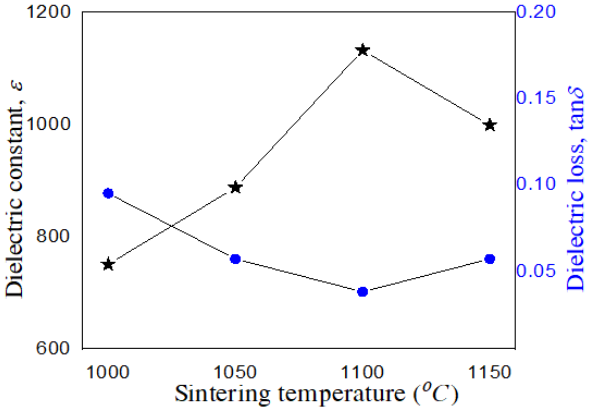

Fig. 4. The dependence of the dielectric constant and the dielectric loss on the sintering temperature

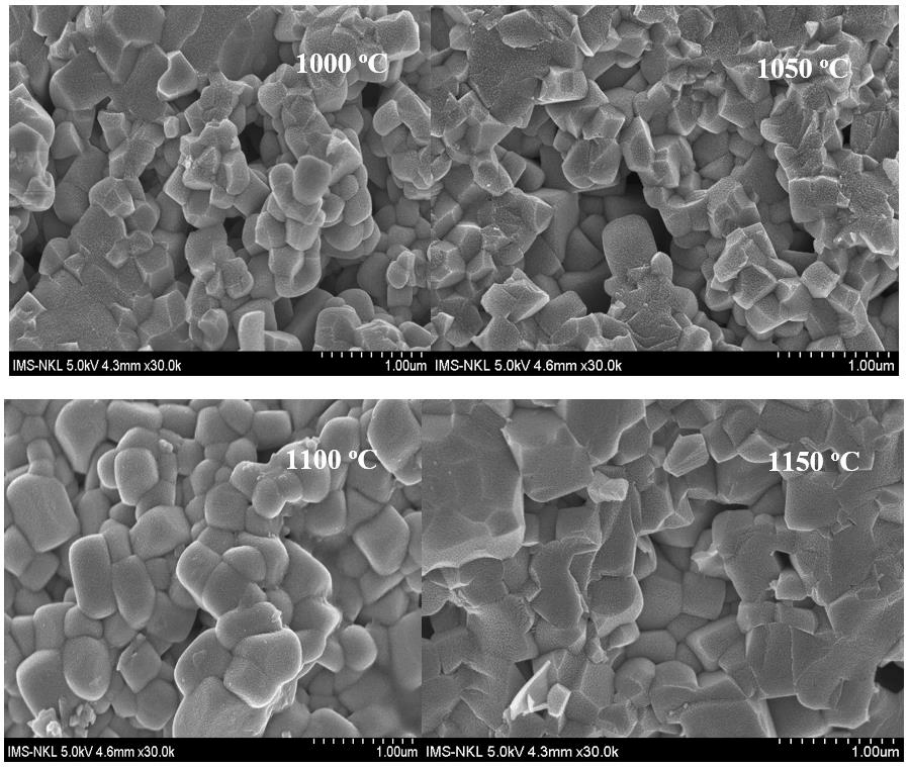

Fig. 5. Surface morphology of $Bi_{0.5}(Na_{0.8}K_{0.2})_{0.5}SnO_3$ ceramics at different sintering temperatures

Fig. 6 shows the X-ray diffraction patterns of BNKS ceramics sintered at 1100 °C. All the samples seem to have a single perovskite structure. The co-existence of rhombohedral and tetragonal phases in the perovskite phase could be analyzed from the XRD patterns with 2θ from 42 to 47°. Several previous publications demonstrate that the transition between rhombohedral and tetragonal phases could be determined by analyzing the peaks $(002)_T$ (tetragonal) and $(200)_R$ at the proximity of 2θ ≈ 44.6° [19]. The division of peaks $(002)_T$ and $(200)_R$ indicates the presence of ferroelectric phase transition [20, 21]. Therefore, we believe that both rhombohedral and tetragonal phases exist in the BNKS crystal. When the potassium content increases, the intensity of peaks $(002)_T$ and $(200)_T$ also increases. The $(002)_T$ and $(200)_R$ double peaks are clearly observed when x = 0.2. This increase can be further clarified through Goldschmidt's tolerance factors.

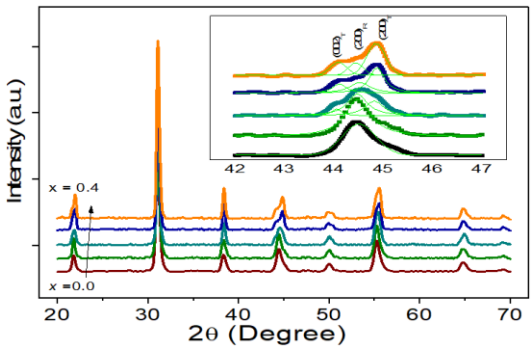

Fig. 6. X-ray diffraction patterns of BNKS ceramics

$$t_{BNKS} = \frac{r_{Bi}+0.5((1-x)r_{Na}+xr_K)+r_O}{\sqrt{2}(r_{Sn}+r_O)} \quad (2)$$

where r is the atomic radius of the element.

When r_{Sn} = 0.055 nm; r_{Bi} = 0.103 nm; r_{Na} = 0.102 nm; r_K = 0.138 nm; and r_O = 0.14 nm, the densification factor (t_{BNKS}) is larger than 1. When x increases, the densification factor increases. This increase would cause crystal deformation and may lead to an enhancement in the ferroelectric and piezoelectric properties of the crystals [22].

pISSN 1859-1388
eISSN 2615-9678

Fig. 7 (a) shows the temperature dependence of the dielectric constant (ε) and the dielectric loss tanδ of the BNKS ceramics sintered at 1100 °C at 1 kHz. This figure shows that this is a relaxer material with the phase transition temperature in the measured temperature range [1]. The dielectric constant increases as x increases, and when x = 0.2, it reaches the maximum value of 4800. This increase might result from the phase transition near the morphology phase boundary [1]. The first transition is ferroelectric-antiferroelectric phase transition occurring at the depolarization temperature (T_d), and the second transition is the antiferroelectric-paraelectric phase transition at a higher phase transition temperature (also known as Curie temperature – T_m) [20, 23]. Fig. 7 (b) shows the dependence of T_d and T_m of BNKS ceramics on the concentration x. As x increases, the T_d temperature decreases from 131 to 97 °C while the T_m temperature increases from 245 to 280 °C.

The P–E hysteresis loops were measured to investigate the ferroelectric properties of BNKS ceramics (Fig. 8a). From these hysteresis loops, the remanent polarization values (P_r) and the coercive field (E_c) were determined (Fig. 8b). The value of P_r reaches a maximum of 11.9 μC/cm² when x = 0.2, and then it decreases gradually. This result is also consistent with the piezoelectric properties investigated in Fig. 9.

To investigate the piezoelectric properties of BNKS ceramics, we recorded the spectra of radial resonance and thick resonance of the samples (Fig. 9). Based on the IRE-61 standard, we calculated the electromechanical coupling factors in the planar mode (k_p) and the thickness mode (k_t).

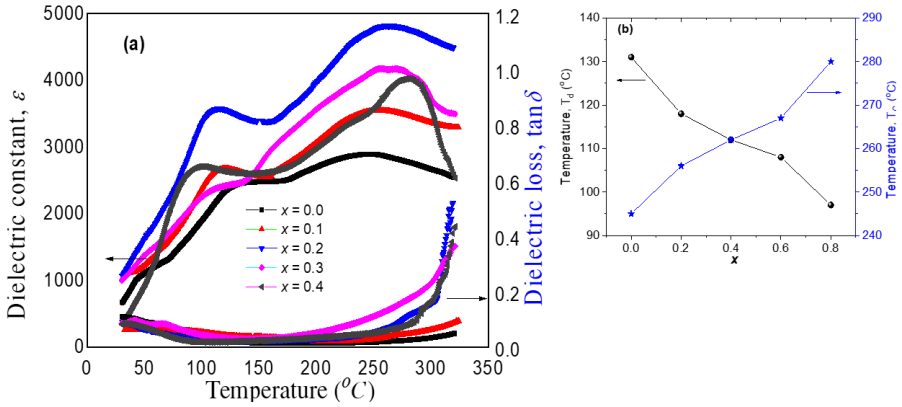

Fig. 7. (a) Temperature dependence of dielectric constant ε and dielectric loss and (b) dependence on the concentration x of two phase-transition temperatures of the BNKS ceramics

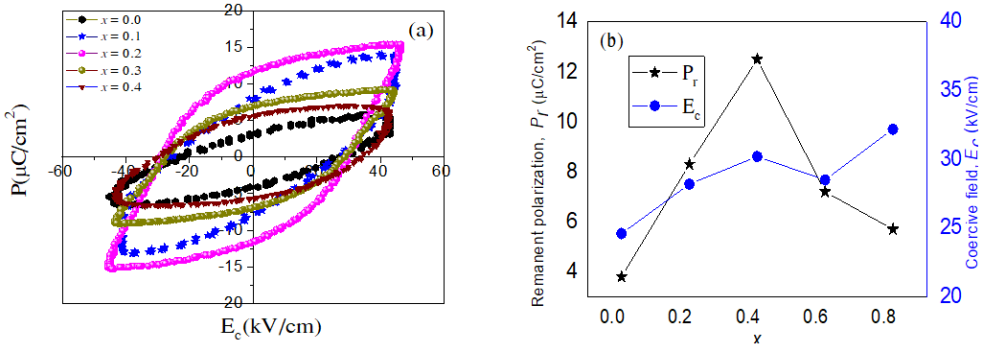

Fig. 8. P–E hysteresis loops of BNKS ceramics measured at room temperature

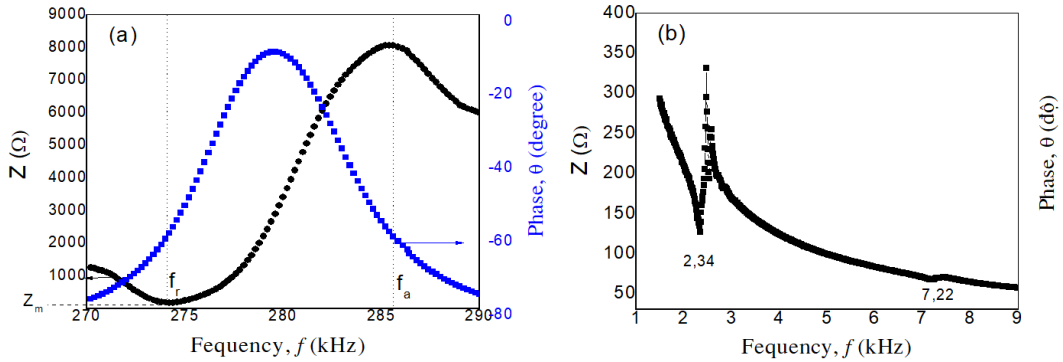

Fig. 9. Spectra of radial resonance (a) and thick resonance (b) of BNKS ceramics

Fig. 10 shows the electromechanical coupling factor (k_p and k_t) and the mechanical quality factor (Q_m) as functions of the concentration x. When $x < 0.2$, k_p, k_t, and Q_m increase rapidly with increasing x. When $x > 0.2$, those values start to decrease. Therefore, the piezoelectric properties are optimized when $x = 0.2$; $k_p = 0.31$; $k_t = 0.27$; and $Q_m = 56$. This is also appropriate to the ceramic density and largest particle size. When BNKS is sintered at a low temperature of 1100 °C and $x = 0.2$, the morphology phase boundary also appears between the tetragonal and rhombohedral phases.

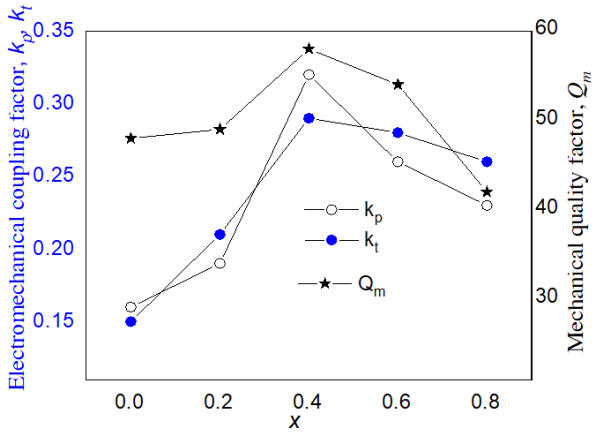

Fig. 10. Electromechanical coupling factors (k_p, k_t) and mechanical quality factor Q_m of BNKS ceramics at room temperature

4 Conclusion

The $Bi_{0.5}(Na_{1-x}K_x)_{0.5}SnO_3$ ceramics, in which x = 0, 0.1, 0.2, 0.3 and 0.4, were fabricated via the conventional solid-state reaction with the help of ultrasound waves in the milling process. The effects of concentration x and sintering temperature on the physical properties of $Bi_{0.5}(Na_{1-x}K_x)_{0.5}SnO_3$ ceramics were investigated. All the samples seem to have a single perovskite structure. The co-existence of rhombohedral and tetragonal phases in the perovskite phase might improve the dielectric properties of the ceramics. The $Bi_{0.5}(Na_{0.8}K_{0.2})_{0.5}SnO_3$ ceramics sintered at 1100 °C show the highest dielectric constant (ε = 1131) at room temperature. This is why the BNKS ceramics can have the remanent polarization of 11.9 μC/cm² and electromechanical coupling factors k_p of 0.31 and k_t of 0.27.

Funding statement

This research was funded by The Ministry of Education and Training of Vietnam under Grant No. B2019-DHH-13.

References

1. Xu Y. Ferroelectric Materials and Their Applications. Amsterdam-London-New York-Tokyo: North-Holland; 1991.

pISSN 1859-1388
eISSN 2615-9678

2. Luan NDT, Vuong LD, Chuong TV, Tho NT. Structure and physical properties of PZT-PMnN-PSN ceramics near the morphological phase boundary. Advances in Materials Science and Engineering. 2014;2014:1-8.

3. Tho NT, Vuong LD. Fabrication and characterization of PZT-PMnN-PSbN ceramics doped with ZnO. Hue University Journal of Science: Natural Science. 2020; 129(1D):5-13.

4. Inoue A, Nguyen TT, Noda M, Okuyama M. Low temperature preparation of bismuth-related ferroelectrics by hydrothermal synthesis. 2007 Sixteenth IEEE International Symposium on the Applications of Ferroelectrics. 2007;136-137.

5. Nguyen TT, Kanashima T, Okuyama M. Leakage current reduction and ferroelectric property of $BiFe_{1-x}Co_xO_3$ thin films prepared by chemical solution deposition using rapid thermal annealing. MRS Proceedings. 2009;1199(1):114-119.

6. Tho NT, Inoue A, Noda M, Okuyama M, Low temperature preparation of bismuth-related ferroelectrics powder and thin films by hydrothermal synthesis. Ferroelectrics and Frequency Control. 2007;54(12):2603-2607.

7. Tho NT, Kanashima T, Sohgawa M, Ricinschi D, Noda M, Okuyama M. Ferroelectric properties of $Bi_{1.1}Fe_{1-x}Co_xO_3$ thin films prepared by chemical solution deposition using iterative rapid thermal annealing in N_2 and O_2. Japanese Journal of Applied Physics. 2010;49(9S):09MB05.

8. Tho NT, Kanashima T, Okuyama M. Leakage current reduction and ferroelectric property of $BiFe_{1-x}Co_xO_3$ thin films prepared by chemical solution deposition using iterative rapid thermal annealing at approximately 520 °C. Japanese Journal of Applied Physics. 2010;49(9R):095803.

9. Truong-Tho N, Nghi-Nhan NT. Fabrication by annealing at approximately 1030 °C and electrical characterization of lead-free $(1-x)Bi_{0.5}K_{0.5}TiO_3$–$xBa(Fe_{0.5}Nb_{0.5})_{0.05}Ti_{0.95}O_3$ piezoelectric ceramics. Journal of Electronic Materials. 2017;46(6):3585-3591.

10. Tho NT. Fabrication and electrical characterization of leadfree $BiFe_{0.91}(Mn_{0.47}Ti_{0.53})_{0.09}O_3$–$BaTiO_3$ ceramics. Hue University Journal of Science: Natural Science. 2020;129(1B):63-70.

11. Kozlenko DP, Dang NT, Madhogaria RP, Thao LTP, Kichanov SE, Tran N, et al. Competing magnetic states in multiferroic $BaYFeO_4$: A high magnetic field study. Physical Review Materials. 2021;5(4).

12. Truong-Tho N, Vuong LD. Effect of sintering temperature on the dielectric, ferroelectric and energy storage properties of SnO_2-Doped $Bi_{0.5}(Na_{0.8}K_{0.2})_{0.5}TiO_3$ lead-free ceramics. Journal of Advanced Dielectrics. 2020;10(04):2050011.

13. Vuong LD, Quang DA, Quan PV, Truong-Tho N. Fabrication of $Bi_{0.5}(Na_{0.4}K_{0.1})TiO_3$ lead-free ceramics using reactive templated grain growth method for improving their preferred degree of orientation, dielectric, and ferroelectric properties. Journal of Electronic Materials. 2020 08 26;49(11):6465-6473.

14. Truong-Tho N, Vuong LD. Sintering behavior and enhanced energy storage performance of SnO_2-modified $Bi_{0.5}(Na_{0.8}K_{0.2})_{0.5}TiO_3$ lead-free ceramics. Journal of Electroceramics. 2020.

15. Vuong LD, Tho NT. The sintering behavior and physical properties of Li_2CO_3-doped $Bi_{0.5}(Na_{0.8}K_{0.2})_{0.5}TiO_3$ lead-free ceramics. International Journal of Materials Research. 2017;108(3):222-227.

16. Vuong LD, Truong-Tho N. Effect of ZnO nanoparticles on the sintering behavior and physical properties of $Bi_{0.5}(Na_{0.8}K_{0.2})_{0.5}TiO_3$ lead-free ceramics. Journal of Electronic Materials. 2017;46(11):6395-6402.

17. Truong-Tho N, Le Vuong D. Study on the strain behavior and piezoelectric properties of lead-free $Bi_{0.5}(Na_{0.8}K_{0.2})_{0.5}TiO_3$ ceramics modified with Sn^{4+} ions. Journal of Materials Science: Materials in Electronics. 2021.

18. Mokhtari O, Nishikawa H. Transient liquid phase bonding of Sn–Bi solder with added Cu particles, Journal of Materials Science: Materials in Electronics. 2016;27(5):4232-4244.

19. Izumi M, Yamamoto K, Suzuki M, Noguchi Y, Miyayama M. Large electric-field-induced strain in $Bi_{0.5}Na_{0.5}TiO_3$–$Bi_{0.5}K_{0.5}TiO_3$ solid solution single crystals. Applied Physics Letters. 2008;93(24): 242903.

20. Wang B, Luo L, Ni F, Du P, Li W, Chen H. Piezoelectric and ferroelectric properties of $(Bi_{1-x}Na_{0.8}K_{0.2}La_x)_{0.5}TiO_3$ lead-free ceramics, Journal of Alloys and Compounds. 2012;526:79-84.

21. Kang SH, Ahn CW, Lee HJ, Kim IW, Park EC, Lee JS. Dielectric and pyroelectric properties of Li_2CO_3 doped $0.2Pb(Mg_{1/3}Nb_{2/3})O_3$–$0.5Pb(Zr_{0.48}Ti_{0.52})O_3$–

0.3Pb($Fe_{1/3}Nb_{2/3}$)O_3 ceramics. Journal of Electroceramics. 2008;21(1-4):855-858.

22. Sasaki A, Chiba T, Mamiya Y, Otsuki E. Dielectric and piezoelectric properties of ($Bi_{0.5}Na_{0.5}$)TiO_3–($Bi_{0.5}K_{0.5}$)TiO_3 systems. Japanese Journal of Applied Physics. 1999;38(Part 1, No. 9B):5564-5567.

23. Yoo J, Lee S. Piezoelectric and dielectric properties of low temperature sintered $Pb(Mn_{1/3}Nb_{2/3})_{0.02}$ $(Ni_{1/3}Nb_{2/3})_{0.12}(Zr_xTi_{1-x})_{0.86}O_3$ system ceramics. Transactions on Electrical and Electronic Materials. 2009;10(4):121-124.